13 Drug–Drug Interactions 1: Inhibition

MURALI SUBRAMANIAN and TIMOTHY S. TRACY
Department of Experimental and Clinical Pharmacology, College of Pharmacy, University of Minnesota, Minneapolis, MN, USA

13.1 INTRODUCTION

Nearly two million adverse drug reactions are reported annually, of which 26% can be attributed to avoidable drug–drug interactions (DDIs) [1]. Predicting potential DDIs is one of the most important activities that a pharmaceutical company undertakes before the approval of any new drug. DDI predictions are primarily governed by elucidation of the metabolism of any new entity. Seventy-three percent of the top 200 drugs are cleared primarily by metabolism, of which 75% of the metabolism occurs due to cytochrome P450 enzymes, a superfamily of oxidative enzymes found mainly in the liver and also distributed in the intestine, kidneys, adrenal glands, lungs, and other organs. Of all the P450 enzymes, CYP3A4, CYP2C9, CYP2C19, and CYP2D6 are responsible for more than 80% of the oxidative metabolism of the top 200 drugs and hence are of special interest to the drug metabolism scientist [1]. Of late, other P450 enzymes such as CYP1A2, CYP2B6, and CYP2C8 have been recognized to be of increasing importance because of an expansion of drugs metabolized by these enzymes, their role in formation of toxic metabolites, and the occurrence of genetic polymorphisms affecting activity.

Although known about for many years, DDIs were generally mild to moderate in severity and could be managed clinically. However, the clinical importance of DDIs truly became front and center with the occurrence of the life-threatening and sometimes fatal interaction of combinations such as terfenadine–ketoconazole and terfenadine–erythromycin, for example, Refs 2–4. In these cases, the potentially fatal arrhythmic condition, Torsades de Pointes, was induced by the coadministration of

Encyclopedia of Drug Metabolism and Interactions, 6-Volume Set, First Edition.
Edited by Alexander V. Lyubimov.

these agents. It was later learned that this interaction was due to a reduced metabolism of the parent drug, terfenadine, which normally undergoes rapid metabolism to a non-cardiotoxic metabolite, fexofenadine. These and similar interactions that have been identified subsequently clearly demonstrated that as medications become more potent, the potential clinical ramifications of a DDI can also become more pronounced.

When more than 25% of the clearance of a given drug is carried out by a single P450 enzyme, there is cause for concern from a DDI perspective [5]. However, a confounding factor in predicting P450-mediated metabolism of a compound is the promiscuous nature of these enzymes, allowing them to catalyze the metabolism of a wide variety of substrates with sometimes overlapping substrate specificity. A practical implication of this is that some drugs may be a substrate to a particular P450 but an inhibitor of another P450. In addition, P450 enzymes tend to be allosteric enzymes and in fact may have two or three catalytic sites within their active site, sometimes necessitating the use of multiple probe substrates for a single enzyme such as CYP3A4. Finally, the interplay of P450 enzymes with other metabolizing enzymes such as uridine diphospho glucuronosyltransferase (UGT) enzymes and glutathione S-transferase (GST) enzymes, and transporters such as P-glycoprotein (P-gp) also serve to confound the prediction of DDIs. Indeed, the US Food and Drug Administration (FDA) has released guidance documents for conducting experiments and clinical studies related to DDIs [6,7]. The focus of this chapter is to elucidate the basic concepts of the various kinds of inhibition of drug-metabolizing enzymes, the equations that can be used to describe the various types of inhibition and the prediction of the *in vivo* inhibition DDIs utilizing *in vitro* data.

13.2 BASIC INHIBITION MECHANISMS

The interaction of two drugs to produce inhibition of single or multiple enzymes can lead to DDIs with clinical consequences. Hence, the determination of a candidate drug's ability to inhibit metabolizing enzymes forms a critical part of drug discovery screens. *In vitro* studies can also help determine a drug's potency to inhibit drug-metabolizing enzymes, typically through determination of the K_i (inhibition constant) or IC_{50} (concentration producing 50% inhibition). Kinetically, enzyme inhibition can be categorized into four main types—competitive, noncompetitive, uncompetitive, and mixed. In addition, irreversible inhibition, also termed *mechanism-based inhibition*, is increasingly being observed (but will be dealt with in another chapter of this series).

The first step in the determination of the ability of a compound to inhibit an enzyme is typically the determination of its IC_{50} toward a particular enzyme–substrate combination. This involves measurement of the turnover of the substrate in the absence and presence of the purported inhibitor. Either fluorescent or luminescent assays have been used in the past for high throughput determinations of IC_{50} values for candidate compounds. Both technologies involve the use of prefluorescent (or preluminescent) substrates that are incubated with recombinant enzymes with and without inhibitor, with the fluorescence or luminescence occurring following metabolism [5] and any decrease in signal as compared to incubations absent, the inhibitor being used as a measure of inhibition. However, lack of isoform specificity (thus, requiring use of expressed enzymes) and sometimes unusually high K_m values for the reaction and frequent occurrence of atypical kinetics with these compounds has greatly limited their

utility. Thus, because of advances in LC-MS/MS technology, use of specific probe substrates and monitoring of metabolite production by mass spectrometric methods has become the standard for inhibition kinetics determinations. Particularly with the speed and resolution of ultra performance liquid chromatography (UPLC) and the selectivity of an LC-MS/MS, minimal method development is required and highly specific substrates can be used to measure turnover. Cassette analysis wherein multiple compounds are dosed together can further enhance throughput, and utilizing robotics for sample processing can automate most of the process. However, again one must be cautious when using cassette methods because of isoform cross-reactivity of compounds.

Commonly, early in the drug discovery process, only IC_{50} values are determined since this requires just one substrate concentration (typically at or near K_m) and incubation of inhibitor at multiple levels with an enzyme source. Compounds exhibiting IC_{50} values less than $1\,\mu M$ are generally considered high risk to cause *in vivo* DDIs, while those exhibiting IC_{50} values greater than $30\,\mu M$ are generally considered to be low risk [8]. Compounds with IC_{50} values between these extremes are of concern and require additional consideration. When conducting *in vitro* inhibition analyses, solubility of inhibitor and substrate are concerns due to the increasing propensity for compounds to be very lipophilic. In this case, nepahlometric methods can be used to assess whether precipitation of compound has occurred [9]. For promising drug candidates that also exhibit a low IC_{50} value toward a particular P450, it may be instructive to conduct additional experiments to determine K_i values (which are independent of substrate concentration) and the mechanism of inhibition. When determining K_i values, initial substrate conditions (turnover less than 10%), substrate not at saturation conditions (which would diminish inhibitory effects), and the possibility of atypical kinetics need to be taken into account.

The FDA recommended list of *in vivo* substrates and inhibitors (as positive controls) include the following substrate and inhibitor pairs, respectively, caffeine and fluvoxamine for CYP1A2, efavirenz and ticlopidine for CYP2B6, rosiglitazone and phenelzine for CYP2C8, *S*-warfarin and fluconazole for CYP2C9, omeprazole and fluvoxamine for CYP2C19, dextromethorphan and quinidine for CYP2D6, chlorzoxazone and disulfiram for CYP2E1, and midazolam and ketoconazole for CYP3A4/3A5 [10]. To accurately determine the type of inhibition and the K_i of the inhibitor require incubations of at least 3–4 concentrations of the substrate (bracketing the K_m) and at least 3–4 concentrations of the inhibitor. In contrast to IC_{50} values, K_i values are independent of substrate and protein concentration. Diagnostic plots, such as the Eadie–Hofstee and Dixon plots, can help determine the nature of the inhibition and give an approximate estimation of the various parameters involved [11]. The various types of *in vitro* systems that can be used have been reviewed in another chapter, but briefly, liver microsomes are considered the gold standard for *in vitro* studies and provide an excellent representation of all the enzymes present in the system. However, it should be recognized that they do not include cytosolic enzymes and transporters as well as several conjugation enzymes. If one suspects these other enzymes or transporters are involved in a compound's metabolism, use of human hepatocytes (fresh or cryopreserved) is likely a more appropriate system [12].

13.2.1 Competitive Inhibition

In competitive inhibition, the substrate and inhibitor directly compete for the catalytic site of the enzyme (Scheme 13.1). Commonly, both the inhibitor and substrate are catalyzed by the enzyme; hence, any two substrates for a single enzyme would be in competitive inhibition. Competitive inhibition (Fig. 13.1) is the most commonly observed type of inhibition and the kinetic scheme for this phenomenon is given in Scheme 13.1.

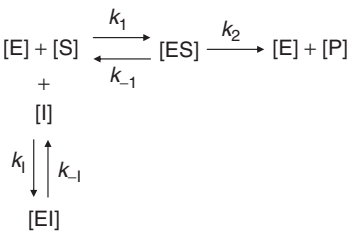

Scheme 13.1

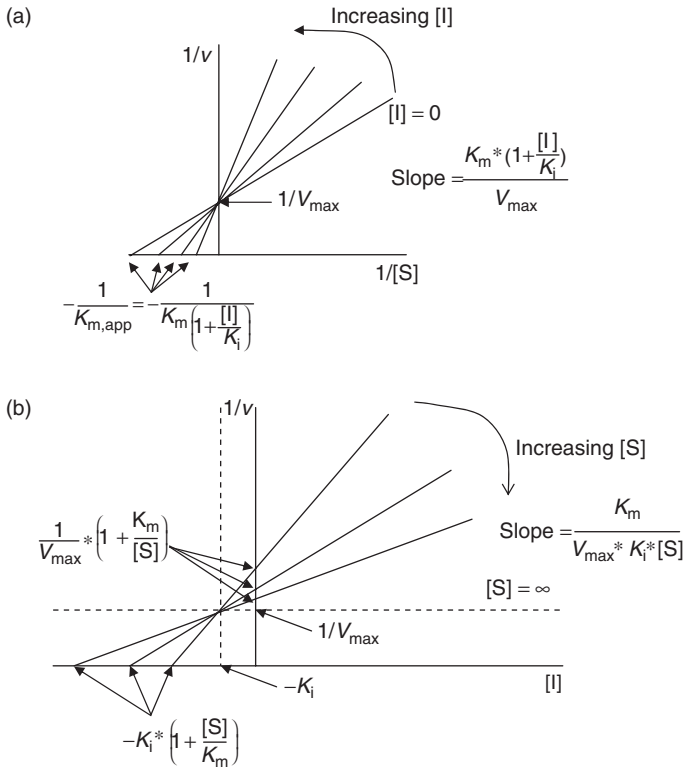

Figure 13.1 Competitive inhibition diagnostics. (a) The EH plot and (b) the Dixon plot. Both the plots can be used to diagnose competitive inhibition and calculate V_{max}, K_m, and K_i.

For the purposes of this chapter, V_{max} and K_m are the Michaelis–Menten kinetic parameters for the substrate in the absence of inhibitor, while $V_{max,\,app}$ and $K_{m,\,app}$ are the parameters in the presence of inhibitor and K_i is the first-order inhibition rate constant (k_{-I}/k_I).

In the case of competitive inhibition, in addition to the usually formed [ES] species, an [EI] species is also reversibly formed. Using a subsaturating concentration of inhibitor and high enough concentration of substrate, maximum (V_{max}) velocities can be obtained. Essentially, at high enough substrate concentrations, the complex shifts away from [EI] and toward [ES], hence V_{max} is unaltered. However, to achieve this shift requires high enough substrate concentrations to offset the inhibitor concentrations; the result being increased K_m. The diagnostic plots for this kind of inhibition are given in Fig. 13.1 [11]. As seen in the Lineweaver–Burk reciprocal plot (Fig. 13.1a), the various fitted lines intersect at the y-axis at $1/V_{max}$, while the x-axis intercept is equal to $1/K_{m,\,app}$. The various slopes and intercepts can be solved to obtain V_{max}, K_m, and K_i. The Dixon plot (Fig. 13.1b) can also be used to diagnose competitive inhibition and to solve for all the kinetic parameters.

From the scheme above, one can derive the kinetic equation for competitive inhibition (Eq. 13.1), which is used to estimate the relevant variables:

$$v = \frac{(V_{max}[S])}{K_m\left(1 + \frac{[I]}{K_i}\right) + [S]} \tag{13.1}$$

where [S] is the substrate concentration and [I] the inhibitor concentration and the other parameters are as described previously.

It is worthy to note that IC_{50} can be directly related to K_i by application of the Cheng–Prusoff Equation [13] (Eq. 13.2):

$$IC_{50} = K_i\left(1 + \frac{[S]}{K_m}\right) \tag{13.2}$$

In this case, if $[S] = K_m$ in the *in vitro* incubations, then $IC_{50} = 2 \times K_i$. Likewise, if $[S] \ll K_m$ (as in *in vivo* situations) then $IC_{50} \approx K_i$.

13.2.2 Noncompetitive Inhibition

In noncompetitive inhibition, the inhibitor can complex with either the free enzyme [E] or an enzyme–substrate complex [ES] to form an unproductive enzyme–substrate–inhibitor [ESI] complex (Scheme 13.2). In addition, the substrate can bind to the enzyme active site even when the inhibitor is already bound to the enzyme. Noncompetitive inhibition occurs when the inhibitor binds to an allosteric location on the enzyme or occupies a spot in the active site exclusive of the catalytic site. This could result in conformational changes in the enzyme or altered substrate binding. For example, curcumin noncompetitively inhibits CYP2C9 and CYP2D6, while olanzapine noncompetitively inhibits CYP2C9 and CYP3A4 [14,15]. The kinetic scheme for noncompetitive inhibition is given in Scheme 13.2.

Since [I] can complex with both [E] and [ES], forming either [EI] or [ESI], increasing the concentration of [S] is inadequate to drive the equilibrium of the reaction all the way toward the [ES] complex. The presence of the unproductive complex, [ESI],

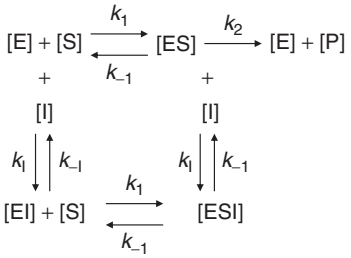

Scheme 13.2

reduces the effective concentration of [ES] and hence reduces the maximum achievable velocity, V_{max}. Since [S] and [I] bind at different sites on the enzyme, the presence of one ligand (either substrate or inhibitor) does not affect the binding affinity of the other, meaning that [S] can bind to both [E] and [EI] with equal affinity. In addition, the [ESI] complex can dissociate to form [ES] plus [I], of which the [ES] complex is then productive. For these reasons, in noncompetitive inhibition, K_m is unchanged [11]. The diagnostic plots for noncompetitive inhibition are shown in Fig. 13.2 [11]. The reciprocal Lineweaver–Burk plot (Fig. 13.2a) has a y-intercept of $1/V_{max,\,app}$, while the x-intercept is $-1/K_m$. All kinetic parameters can be determined by solving for the intercepts and slope. The K_i can also be obtained from the Dixon plot (Fig. 13.2b).

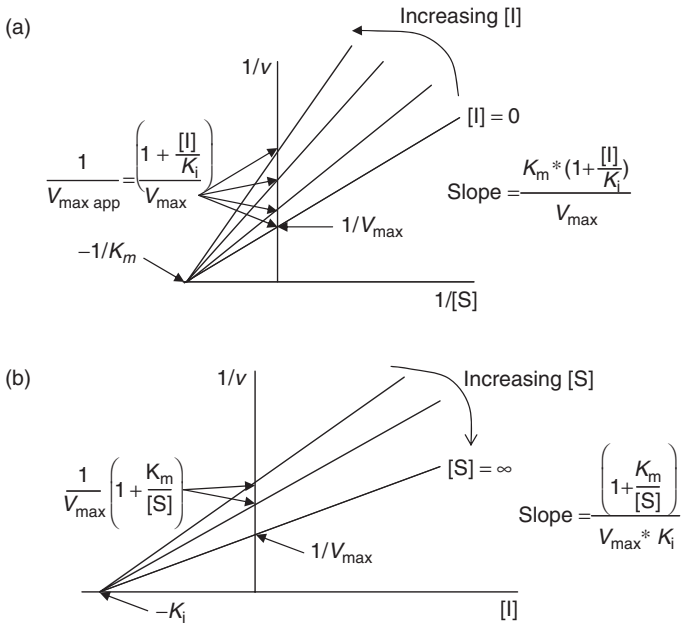

Figure 13.2 Noncompetitive inhibition diagnostics. (a) The EH plot and (b) the Dixon plot. Both the plots can be used to diagnose competitive inhibition and calculate V_{max}, K_m, and K_i.

The equation for noncompetitive inhibition is given below [11]:

$$v = \frac{V_{max}[S]}{K_m\left(1 + \frac{[I]}{K_i}\right) + [S]\left(1 + \frac{[I]}{K_i}\right)} \tag{13.3}$$

In this case, IC_{50} is related to K_i by the following equation:

$$IC_{50} = K_i \tag{13.4}$$

13.2.3 Uncompetitive Inhibition

In uncompetitive inhibition, the inhibitor binds only to the [ES] complex resulting in the formation of a catalytically inactive [ESI] complex (Scheme 13.3). Since substrate-bound enzyme is required to make the enzyme amenable to inhibitor binding, the inhibitor cannot directly bind to the enzyme itself without substrate being present [11]. Uncompetitive inhibition is rarely observed exclusively and when observed, usually occurs in association with other types of inhibition. However, examples of this kind of inhibition have been observed with the drug-metabolizing enzymes. For example, meloxicam uncompetitively inhibits quinidine metabolism by CYP3A4 [16]. The kinetic scheme for uncompetitive inhibition is given in Scheme 13.3.

Since [I] binds to [ES] forming an unproductive [ESI] complex, the addition of excess substrate is insufficient to convert all the [ESI] complexes to [ES] complexes, resulting in a reduction in V_{max}. However, since [I] reacts with [ES] forming [ESI], thereby depleting the [ES] pool, the forward reaction of [E] + [S] is favored and thus, likewise, K_m values are also decreased [11]. The diagnostic plots for uncompetitive inhibition are presented in Fig. 13.3 [11]. The Lineweaver–Burk reciprocal plot is (Fig. 13.3a) characterized by parallel lines with y-intercepts of $1/V_{max,\,app}$ and x-intercepts of $-1/K_{m,\,app}$. The Dixon plot (Fig. 13.3b) can be used to directly obtain K_i.

The equation for uncompetitive inhibition (Eq. 13.5) is given below:

$$v = \frac{V_{max}[S]}{K_m + [S]\left(1 + \frac{[I]}{K_i}\right)} \tag{13.5}$$

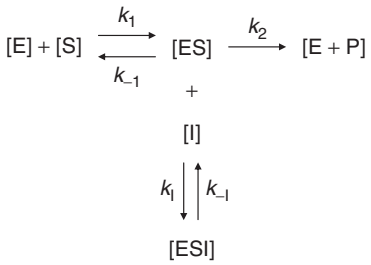

Scheme 13.3

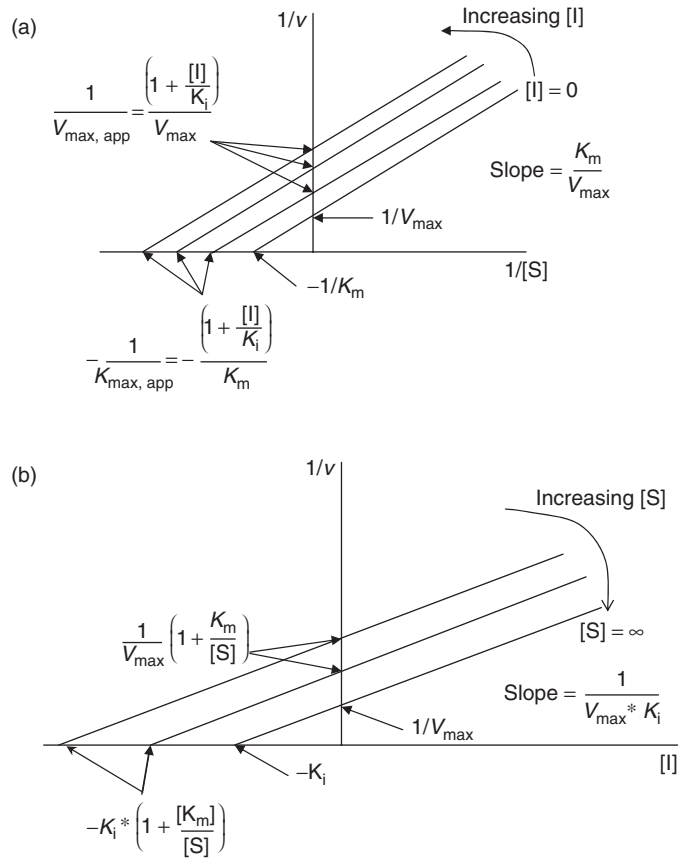

Figure 13.3 Uncompetitive inhibition diagnostics. (a) The EH plot and (b) the Dixon plot. Both the plots can be used to diagnose competitive inhibition and calculate V_{max}, K_m, and K_i.

For uncompetitive inhibition, IC_{50} is related to K_i by the following equation:

$$IC_{50} = K_i\left(1 + \frac{K_m}{[S]}\right) \tag{13.6}$$

In this case, if $[S] = K_m$ then $IC_{50} = 2^*K_i$ and if $[S] \ll K_m$ (as is typical of *in vivo* situations) then $IC_{50} \gg K_i$, meaning that *in vivo*, even if the inhibitor exhibits a low K_i, achieving 50% inhibition is unlikely because of low [S] concentrations [13].

With competitive inhibition, IC_{50} values are dependent on the substrate concentration employed and are usually higher than K_i values (and thus, the higher the substrate concentration, the higher the IC_{50} since the inhibitor has to compete with substrate for the active site). In the case of uncompetitive inhibition, the scenario is reversed. Since the inhibitor can only bind the enzyme after the substrate has bound to the enzyme, increasing the substrate concentrations leads to lowering of the IC_{50}. For noncompetitive inhibition, the inhibitor binds to the enzyme at a site different from the substrate-binding site, and this binding is independent of whether the substrate is

bound to the enzyme. Hence, for noncompetitive inhibition, IC_{50} is independent of substrate concentrations [13].

13.2.4 Mixed Inhibition

Mixed inhibition is for the most part a special case of noncompetitive inhibition, wherein the dissociation constants for the formation of [ES], [EI], [ESI] (formed from [ES] + [I] and [EI] + [S]), and [IE] (in cases wherein the formation of [IE] precludes further [S] binding) are different. The discussions of these various kinds of inhibition are beyond the scope of this chapter.

13.3 *IN VITRO–IN VIVO* CORRELATIONS FOR DRUG–DRUG INTERACTIONS: EXPERIMENTAL AND THEORETICAL FACTORS

13.3.1 *In Vitro–In Vivo* Correlations for Drug–Drug Interactions

Being able to predict DDIs on the basis of *in vitro* IC_{50} and K_i data is extremely important to pharmaceutical companies developing drugs. The ability to accurately accomplish this would allow for identification of DDI-based liabilities at an early stage. To this end, many groups have proposed *in vitro–in vivo* correlations based on drug metabolism kinetic theory and tested the equations for success in predicting clinical DDIs [17–26]. Success is usually measured by comparing predicted DDIs with values obtained from clinical trials. While the basic principles of predicting DDIs using *in vitro–in vivo* extrapolations (IVIVEs) has remained unchanged, the methodology has constantly been refreshed. Incorporation of various sources of data (microsomes, hepatocytes, *in vivo* data), allowances for the critical inhibitor concentration, inclusion of protein binding, evaluating the role of the intestine in mediating DDIs and other factors have greatly expanded the utility of this work. This section discusses highlights of the vast literature in this area with a view toward the basic tenets underlying each approach. While these approaches were first developed for P450 enzymes, they can be applied to any drug-metabolizing enzyme, such as UGT enzymes [27].

Most drugs are either competitive or noncompetitive inhibitors of P450 enzymes; hence, the vast majority of literature uses Equations 13.1 and 13.3 to assess the effect of an inhibitor on a drug's disposition when calculating intrinsic clearance of the drug when given with an inhibitor. In the following derivations, it is assumed that the inhibitor does not affect the fraction absorbed from the intestine and the protein binding of the drug (i.e., free fraction stays the same). In addition, the well-stirred model is usually applied to model systemic clearance and is assumed below, as well. Finally, it is also assumed that Michaelis–Menten kinetics is also exhibited by the drug of interest, that is, a V_{max} and K_m can be obtained, and when $[S] \ll K_m$, $[S] + K_m \cong [S]$. When Michaelis–Menten kinetics is not applicable, such as in the case of atypical kinetics that can be observed with most P450 enzymes (although most commonly with CYP3A4 and CYP2C9), one has to make additional allowances. In this case (atypical kinetics), the K_m and V_{max} values of the relevant catalytic site (usually the higher affinity or smaller K_m) as determined by estimation using the appropriate atypical kinetic equation should be applied.

Assuming a drug is cleared by two P450 enzymes, with a fraction metabolized by the primary enzyme (f_{m1}), the intrinsic clearance of the drug from *in vitro* data, Cl_{int} is estimated as in the following Equation 17:

$$Cl_{int} = \frac{V_{max\,1}}{K_{m1}} + \frac{V_{max\,2}}{K_{m2}} = f_{m1}Cl_{int} + (1 - f_{m1})Cl_{int} \tag{13.7}$$

where $V_{max\,1}$ and $V_{max\,2}$ and K_{m1} and K_{m2} are the Michaelis–Menten parameters for enzymes 1 and 2, respectively. The clearance in the presence of the inhibitor (which inhibits only the primary enzyme), $Cl_{int,\,i}$, at concentration [I] and using the inhibition rate constant K_i is then given by the following equation:

$$Cl_{int,i} = \frac{V_{max\,1}}{K_{m1}\left(1 + \frac{[I]}{K_i}\right)} + \frac{V_{max\,2}}{K_{m2}} = \frac{f_{m1}Cl_{int}}{1 + \frac{[I]}{K_i}} + (1 - f_{m1})Cl_{int} \tag{13.8}$$

The ratio of intrinsic clearances (Eq. 13.9) and the ratio of the areas under the curve (AUC, measure of exposure) (Eq. 13.10) are then given by

$$\frac{Cl_{int,i}}{Cl_{int}} = \frac{f_{m1}}{1 + \frac{[I]}{K_i}} + (1 - f_{m1}) \tag{13.9}$$

and

$$\frac{AUC_i}{AUC} = \frac{1}{\frac{f_{m1}}{1+\frac{[I]}{K_i}} + (1 - f_{m1})} \tag{13.10}$$

where AUC and AUC_i are the areas under the curve in the absence and presence of inhibitor. Equation 13.10 is frequently referred to as the *Rowland–Matin equation* [28]. When only one enzyme is responsible for the metabolism of a drug, that is, $f_m = 1$, the equation reduces to (for competitive and noncompetitive inhibition) the following equation:

$$\frac{AUC_i}{AUC} = 1 + \frac{[I]}{K_i} \tag{13.11}$$

When two P450 enzymes are inhibited by an inhibitor, with inhibition rate constants of K_{i1} and K_{i2} for inhibitors 1 and 2 respectively, then the equation becomes

$$\frac{AUC_i}{AUC} = \frac{1}{\frac{f_{m1}}{1+\frac{[I]}{K_{i1}}} + \frac{(1-f_{m1})}{1+\frac{[I]}{K_{i2}}}} \tag{13.12}$$

For uncompetitive inhibition, Equation 13.11 becomes

$$\frac{AUC_i}{AUC} = 1 + \left(\frac{[S]}{K_m}\right)\left(1 + \frac{[I]}{K_i}\right) \tag{13.13}$$

A close examination of Equation 13.10 reveals that successful prediction of DDIs requires confident estimates of [I], K_i, and f_m. While K_i can be reasonably well

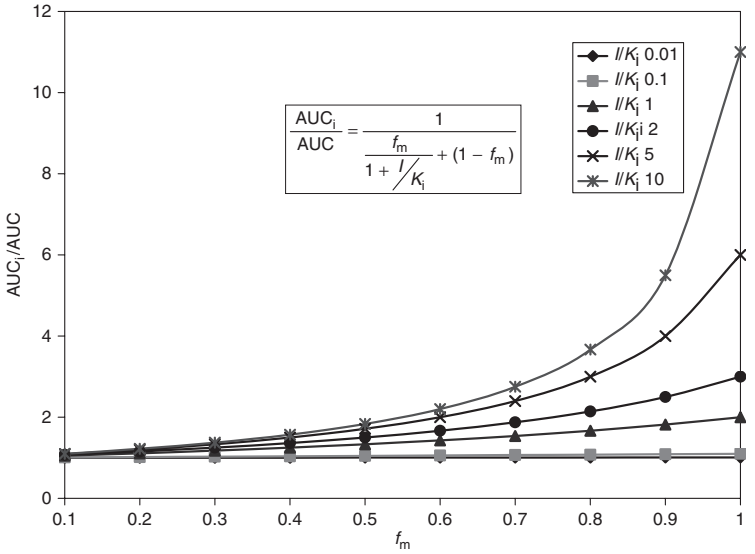

Figure 13.4 Role of f_m and I/K_i in AUC changes on inhibition. As seen, when $f_m < 0.5$, the AUC change will not be greater than twofold, hence will not have clinical significance. Also, when I/K_i is less than 2, the AUC ratio changes are not significant.

estimated from *in vitro* studies, and f_m can be determined with some measure of confidence from *in vitro* systems, considerable uncertainty exists about the value of the appropriate inhibitor concentration that will be relevant at the enzyme active site *in vivo*. Figure 13.4 gives a graphical representation of the role of f_m and the ratio $[I]/K_i$ in the AUC change. As seen, if $f_m < 0.5$ then the increase in AUC at even an infinite concentration of inhibitor will never be greater than twofold. Looking at this relationship from a different perspective, if $[I]/K_i$ is less than 2 then even a twofold increase in AUC is only observed when f_m is greater than 0.75. Hence, if $f_m < 0.5$, or if $[I]/K_i < 2$, then the possibility of a twofold AUC change is minimal.

Using the above methodology, generated *in vitro* data were compared to reports of *in vivo* DDIs culled from 193 studies published in the literature involving CYP2C9, CYP2D6, and CYP3A4/5 [18]. Three inhibitor concentrations were evaluated for their degree of contribution to the accuracy of predications: systemic average inhibitor plasma concentration ($[I]_{avg}$) after repeated oral administration, maximum inhibitor hepatic input concentration ($[I]_{in}$), and maximum inhibitor systemic plasma concentration after repeated oral administration ($[I]_{max}$). The equations used in estimating these three inhibitor concentrations are listed below as derived by Ref. 29:

$$[I]_{avg} = \frac{\left(\frac{D}{\tau}\right)}{\left(\frac{Cl}{F}\right)} \tag{13.14}$$

$$[I]_{max} = \frac{[I]_{avg} k\tau}{1 - \exp(-k\tau)} \tag{13.15}$$

$$[I]_{in} = [I]_{avg} + \frac{k_a F_a D}{Q_h} \tag{13.16}$$

where D and τ are the dose and the dosing interval, respectively, of inhibitor used in the *in vivo* interaction study, k is the elimination rate constant, k_a is the absorption rate constant, F_a is the fraction absorbed from gut into the portal vein, Q_h is the hepatic blood flow rate, and Cl/F is the oral clearance of the victim drug. The values of k_a, F_a, Q_h, and RB (blood-to-plasma concentration ratio) were assumed by these authors to be $0.1\,\text{min}^{-1}$, 1, 1610 mL/min, and 1, respectively. Unbound [I] concentrations were also calculated by multiplying [I] by the free fraction of inhibitor (f_u). The fraction metabolized (f_m) term was not included in these analyses, hence, the underlying assumption is that $f_m = 1$.

It is generally assumed that only free drug or inhibitor is available to exert its effect. However, in these simulations, the use of unbound inhibitor concentration did not always result in the best predictions. In this case, the use of unbound [I] resulted in a number of false negatives. It was observed that $[I]_{max}$ and $[I]_{avg}$ provided similar degrees of accuracy in the predictions, while use of $[I]_{in}$ resulted in the most accurate predictions. When $[I]_{avg}$ was used, accuracy of the predictions was 74%, with 7% false positives and 19% false negatives. When $[I]_{avg,u}$ was used, accuracy of the predictions was 59%, with 5% false positives and 36% false negatives. In these latter two cases, fewer accurate predictions, and a higher degree of false negatives were observed, mainly because the [I] values were lower. When $[I]_{max}$ was used, accuracy of the predictions was 70%, with 9% false positives and 21% false negatives. When $[I]_{in}$ was used, accuracy of the predictions was 69%, with 29% false positives (mainly from CYP2D6 interactions) 2% false negatives. Hence, false negatives were almost completely eliminated when $[I]_{in}$ was used; however, the number of false positives was increased.

In a subsequent analysis, it was observed that the use of hepatic input concentration ($[I]_{in}$) resulted in the best balance between positive and negative interactions and, most importantly, eliminated false negatives [17]. It was also noted that there was a high incidence of false positive predictions, and many true positives were substantially overpredicted when multiple pathways were present and f_m was not included in the AUC equation. Subsequent inclusion of f_m helped reduce the number of false positives, and increased the success in predicting positive or negative interactions increased from 54% to 84%.

Another model for prediction of inhibition DDIs reported that use of $[I]_{avg}$ provided the most accurate predictions [20] and resulted in the highest number of predictions within twofold of *in vivo* AUC_i/AUC. This work also reported a corresponding reduction in bias and an increase in precision when $[I]_{avg}$ was used compared with either $[I]_{in}$ or $[I]_{in,u}$ for a subset of 45 *in vivo* studies. In this case, predictions of AUC ratios for only 9% of the studies were outside twofold of actual when $[I]_{avg}$ was included in the predictive model, compared with 24% and 60% outliers for predictions in which either $[I]_{in}$ or $[I]_{in,u}$ were, respectively, included. Overall, the use of the refined data significantly improved the prediction accuracy by 16% and 35% for predictions based on $[I]_{in}$ and $[I]_{avg}$, respectively, but use of $[I]_{in,u}$ or $[I]_{avg,u}$ worsened predictions. The use of $K_{i,u}$ was also found to improve predictions. It seems unusual that unbound K_i improves predictions, whereas total [I] are associated with improved predictions. It is unclear why this paradox is observed.

Obach and coworkers also published a comprehensive evaluation of the correlation of *in vitro* predictions and *in vivo* data [21]. In this examination, estimations of K_i and IC_{50} values for drug–substrate combinations conducted in human liver

microsomes were made for CYP1A2, CYP2C9, CYP2D6, CYP3A4, and CYP2C19 enzymes, which together account for most of the observed P450 metabolism *in vivo*. The IC_{50} values of inhibitors toward all the P450 enzymes were rank ordered to determine the propensity of an inhibitor for causing inhibition *in vivo*. This *in vitro* rank order was then compared against similarly ranked *in vivo* data. In only 3 of 21 cases, the *in vitro* IC_{50} rank ordering did not correlate with the rank ordering of the *in vivo* data. An initial comparison of IC_{50} data versus *in vivo* DDIs found that inhibitors with an *in vitro* IC_{50} of less than $1\,\mu M$ were more likely to cause a twofold increase in AUC [21]. Among inhibitors with an *in vitro* IC_{50} of more than $1\,\mu M$, only 3 of 44 inhibitors resulted in a twofold or higher AUC change *in vivo*. Conversely, only two drugs that exhibited an *in vitro* IC_{50} of less than $1\,\mu M$ did not result in at least twofold AUC change *in vivo*. However, the IC_{50} requirement of $1\,\mu M$ was found not to apply in the case of mechanism-based inhibitors. These same authors also reported that unbound hepatic inlet inhibitor concentration, in general, provided the best estimates of change in AUC.

More recently, a new approach to predict DDIs utilizing *in vivo* data has been recently proposed [26]. Potential uncertainty introduced by atypical kinetics, mechanism-based inhibitors, and inability to accurately assess the contribution of intestinal metabolism from *in vitro* data are frequently reasons that *in vitro–in vivo* correlations of DDI predictions are not always successful. In an attempt to overcome these shortcomings, in the work of Ohno *et al*., an apparent inhibition ratio (IR) and contribution ratio (CR), analogous to K_i and f_m, respectively, were defined. Since the largest amount of *in vivo* data were available for CYP3A4, this study examined the feasibility of this approach for that isoform only.

In this work, the CR was determined by the following equation:

$$CR_{CYP3A4} = \frac{Cl_{int,CYP3A4}}{Cl_{int}} \tag{13.17}$$

where $Cl_{intCYP3A4}$ is the *in vivo* intrinsic clearance mediated by CYP3A4 and Cl_{int} the total *in vivo* intrinsic hepatic clearance. Compounds with a CR of 1 are fully metabolized by CYP3A4, while those with lower values of CR are metabolized by other isoforms (lower the CR, the greater the contribution by other isoforms).

An IR was also calculated from *in vivo* data using the following equation:

$$IR_{CYP3A4} = \frac{[I_{app}]}{[I_{app}] + K_i} \tag{13.18}$$

where $[I_{app}]$ is the apparent time-average unbound liver concentration. Under these conditions, an IR of 1 represents the lowest possible value of K_i and hence the most potent CYP3A4 inhibitor. Values of IR less than 1 signify less potent CYP3A4 inhibitors (lower the IR, the less potent the inhibitor).

The AUC change (for reversible inhibition) is then given by the above equation:

$$\frac{AUC_i}{AUC} = \frac{Cl_{oral} \cdot F_a}{Cl_{oral,i} \cdot F_a} = \frac{Cl_{int}}{Cl_{int,i}} = \frac{1}{1 - CR_{CYP3A4} \cdot \frac{[I_{app}]}{[I_{app}]+K_i}}$$

$$= \frac{1}{1 - CR_{CYP3A4} \cdot IR_{CYP3A4}} \tag{13.19}$$

This equation essentially resembles Equation 13.10 correlating AUC change with f_m and [I]/K_i.

In this study, the IR and CR were calculated from 53 *in vivo* data sets, beginning with the assumption that simvastatin exhibited a CR of 1. From the *in vivo* AUC change for simvastatin interactions, the IR for the various inhibitors was calculated. This sequential approach was subsequently applied to 60 data sets to determine the CR and IR for 14 substrates and 18 inhibitors, respectively.

A portion of the data was then used as the training set to estimate CR and IR, while the remaining data set was used to check the accuracy of the predictions. The AUC ratio change was predicted within 67–150% for 50 of the studies (83%) and within 50–200% (twofold) for 57 of the studies (90%) [26]. However, this approach only works if the IR and CR of the inhibitor and the substrate are within the calculated list, meaning that *in vivo* clinical data are needed for this calculation. Thus, only the interaction potential of combinations of substrates and inhibitors from the list can be predicted. However, since the list includes 14 substrates and 18 inhibitors, a total of 252 DDIs can be predicted. However, to use this approach for new chemical entities, additional work and testing will be needed since no *in vivo* data for these compounds would exist.

An expanded review of the above work was conducted to correlate IR with K_i and CR with f_m [24]. *In vivo* and *in vitro* CR (f_m) were highly correlated and 29 of 38 combinations sets were within 50–200% when making the *in vitro* to *in vivo* CR comparison. Because of this correlation, once an *in vivo* CR is determined for a new chemical entity, then its potential for DDIs with the original set of 18 inhibitors described by Ohno *et al*. [26] can be predicted with some degree of confidence. However, the potential for DDIs with an inhibitor from outside of this list would be outside the scope of this method's predictive capabilities. IR values, however, were not well correlated with *in vitro* K_i values. Similarly, the [I] concentration used (systemic unbound, systemic total, systemic maximum, or portal vein unbound concentration) also did not make a significant difference in the predictive abilities of the model. IR was correlated with dose/K_i. The authors did propose that if one used a substrate with a known CR, then a clinical trial could be conducted, wherein the new chemical entity (NCE) is the inhibitor. From this trial, IR values for the NCE can be determined and compounds with high IR values then would be flagged for additional studies.

13.3.2 Role of Intestinal Metabolism

When a drug is taken orally, it may be subject to presystemic metabolism in the intestine. While CYP3A4 is the most prevalent P450 in the gut, other important enzymes such as CYP2C9 and the UGT enzymes are also present. In addition, transporters such P-gp are also present in the intestine. P-gp is present in the apical (luminal) side of mature intestinal enterocytes, while CYP3A4 is present in the cytoplasm of the intestinal mucosal enterocytes. Drugs that escape the efflux action of P-gp and the metabolic action of CYP3A4 enter the portal vein, wherein they can undergo metabolism by the liver CYPs and other drug-metabolizing enzymes. For some drugs, this degree of presystemic metabolism or efflux in the gut can comprise a substantial fraction of the overall metabolism, thus preventing their systemic uptake. For example, 57% of orally dosed midazolam is lost due to intestinal metabolism [30], and the liver extraction ratio and intestinal extraction ratio are almost the same (0.44 vs 0.43) [31]. Coadministration

of grapefruit juice with compounds is a convenient experiment that can be performed to determine the contribution of the intestine to clearance of a drug, since grapefruit juice reversibly and irreversibly inhibits CYP3A4 in the intestine [32].

Another indicator of the occurrence of gut metabolism is when the fold change in AUC_{oral}/fold change in AUC_{IV} with and without the inhibitor is greater than 1 [33]. In intravenous (IV) dosing with and without inhibitor, only hepatic clearance is affected by the inhibitor, while during oral dosing with and without inhibitor, both hepatic and first pass (absorption and intestinal metabolism) are affected. Hence, the ratio of oral AUC to IV AUC provides a measure of the effect of the inhibitor on first pass clearance. Ratios of up to 2.8 have been observed, indicating significant gut metabolism. However, in addition to inhibiting P450 enzymes, some inhibitors also inhibit P-gp or other transporters, thereby altering absorption [33]. Hence, the fraction absorbed of the drug also needs to be factored into gut-mediated clearance considerations.

Developing correlations for intestinal *in vitro–in vivo* correlations for DDIs have been an area of substantial study. Since CYP3A4 is the main enzyme responsible for metabolism in the gut, most correlation attempts have focused on inhibition of this important isoform. Since the principles of inhibition and intrinsic clearance remain the same (V_{max}/K_m is constant for CYP3A4 irrespective of its location), the basic equation governing the ratio of intestinal clearances is analogous to the equation for hepatic clearance (Eq. 13.20) [21]:

$$\frac{\mathrm{Cl}_{\mathrm{int,g,i}}}{\mathrm{Cl}_{\mathrm{int,g}}} = \frac{1}{1 + \frac{[\mathrm{I}]_g}{K_i}} \tag{13.20}$$

where $[I]_g$ is the estimated concentration of the inhibitor in the intestinal wall during absorption and is estimated from Equation 13.21. $Cl_{int,g,i}$ and $Cl_{int,g}$ are the intestinal intrinsic clearances in the presence and absence of inhibitor, respectively. K_i is the inhibition rate constant in the gut.

The inhibitor concentration is estimated by application of the following equation [21]:

$$[\mathrm{I}]_g = \frac{Dk_a F_a}{Q_g} \tag{13.21}$$

where F_a is the fraction absorbed, k_a the absorption rate, D the dose, and Q_g the enterocytic blood flow rate (0.3 L/min average). F_g, the intestinal bioavailability, is a function of the intestinal clearance [34] (Eq. 13.22):

$$F_g = \frac{A}{A + \mathrm{Cl}_{\mathrm{int,g}}} \tag{13.22}$$

where A is the absorption constant, assumed to be unaffected by the presence of inhibitors.

The F_g ratio is then determined by the following equation [34]:

$$\frac{F_{g,i}}{F_g} = \frac{A + \mathrm{Cl}_{\mathrm{int,g}}}{A + \mathrm{Cl}_{\mathrm{int,g,i}}} = \frac{1}{F_g + (1 - F_g)\left(\frac{\mathrm{Cl}_{\mathrm{int,g,i}}}{\mathrm{Cl}_{\mathrm{int,g}}}\right)} \tag{13.23}$$

where $F_{g,i}$ and F_g are the intestinal bioavailability in the presence and absence of inhibitor.

Combining these equations, estimation of the change in AUC due to inhibition, incorporating both intestinal and hepatic effects is given by the following equation [21]:

$$\frac{AUC_i}{AUC} = \frac{\left(\frac{Cl_{int}}{F_g}\right)}{\frac{Cl_{int,i}}{F_{g,i}}} = \frac{F_{g,i}}{F_g}\frac{Cl_{int}}{Cl_{int,i}} = \frac{F_{g,i}}{F_g}\frac{1}{\left(\frac{f_{mCYP3A}}{1+\left(\frac{[I]_{in\ vivo}}{K_i}\right)}\right) + \left(1 - f_{mCYP3A4}\right)} \tag{13.24}$$

where AUC_i and AUC are the area under curves in the presence and absence of inhibitor and $Cl_{int,i}$ and Cl_{int} are the intrinsic hepatic clearances in the presence and absence of inhibitor. $[I]_{in\ vivo}$ is the systemic or hepatic inhibitor concentration and $f_{mCYP3A4}$ is the fraction metabolized by CYP3A4, since CYP3A4 is the predominant enzyme causing intestinal metabolism.

The ratio of $F_{g,i}/F_g$ must be determined from *in vivo* studies using both IV and oral dosing, in the presence and absence of inhibitors [33]. Such data sets are rare. However, the ratio can also be determined by substituting Equation 13.22 into Equation 13.24. F_g and F_h have to be determined from *in vivo* studies in anhepatic patients or from a combination of *in vitro* and *in vivo* studies [33,34]. Galetin and coworkers have compiled F_g values for 25 drugs [33]. The requirement of having *in vivo* data makes predicting intestinal DDIs more challenging than predicting hepatic DDIs.

With all of this said, the actual value of including intestinal metabolism in DDI predictions remains unclear. One study found that when the physiologically relevant unbound hepatic inlet concentration was used, ignoring the intestinal component of metabolism increased the error [21]. However, another study involving cases of time-dependent inhibition observed that the percentage of cases where predictions were within twofold accuracy actually declined from 90% to 70% when an intestinal component was considered [33]. Another study found that utilization of the intestinal component did not improve or in some cases, worsened the predictions [20]. Predictions were found to the most accurate (with and without incorporation of intestinal component) for compounds with high intestinal bioavailability (low first pass metabolism, high F_g).

13.3.3 Role of Fraction Metabolized (f_m)

The fraction of the substrate metabolized by a given enzyme (f_m) is another key parameter included in the successful prediction of DDIs from *in vitro* data (Eq. 13.10). Hence, accurate estimation of f_m is critical to the quality of the prediction. Fortunately, f_m can generally be estimated from *in vitro* reaction phenotyping studies, wherein the substrate is incubated with individual recombinant P450 enzymes and the relative contribution of each P450 to the metabolism of the substrate is determined. A more realistic determination of f_m can be obtained from HLMs with and without specific P450 inhibitors. In addition, studies have also used *in vivo* metabolism

data to determine f_m. For example, the role of CYP2D6 in the metabolism of a substrate can be obtained by comparing poor metabolizers with extensive metabolizers [19]. Comparing the formation clearance of metabolites measured in the urine also provides the contribution of an enzyme in formation of a metabolite, provided that metabolite is formed by a single enzyme. Obviously, if multiple enzymes produce a common metabolite, then formation clearances from urine data will be of limited value. The change in f_m in the presence of the inhibitor can also be determined by this technique.

One of the common assumptions made in determining AUC changes due to enzyme inhibition is that f_m remains essentially constant for a certain drug–enzyme combination. However, f_m may vary depending on substrate concentration if K_m is substantially exceeded. At higher substrate concentrations, enzymes with larger K_m values may make a greater contribution to the drug's metabolism than would be the case at lower substrate concentrations. In addition, interindividual variation in terms of individual polymorphisms and variability in quantity of enzymes may also affect f_m values. Hence, an additional complicating factor in DDI predictions is that f_m can vary through the course of the experiment.

Several studies have examined the utility of including an f_m term in their DDI predictions from *in vitro* data [17,19]. Brown *et al*. observed that the number of predictions within twofold of actual increased from 54% to 84% when f_m was incorporated [19]. The percentage of estimations overpredicting changes in AUC decreased from 46% to 15% and the percentage of underpredictions changed from 0% to 1%. Hence, the improvement was due to the reduction in overpredictions which makes intuitive sense, because when f_m is not incorporated in the equation, the underlying assumption is that $f_m = 1$. This generally overestimates the contribution of an individual enzyme, leading to overprediction of DDI potential, when multiple enzymes may in fact be involved [19].

13.3.4 Role of Genotype

A small number of clinical trials have examined the role of genotype in DDIs. Since *in vitro* studies have demonstrated that various polymorphic variants of drug-metabolizing enzymes can be inhibited to different extents, even while employing the same substrate and inhibitor, clinical trials were performed to determine if this effect persisted *in vivo*. For example, when the CYP2C9 inhibitor fluconazole was administered to steady state (400 mg q.d. for 7 days) and then flurbiprofen (a CYP2C9 substrate) was coadministered, individuals with the CYP2C9*1/*1, CYP2C9*1/*3, and CYP2C9*3/*3 genotypes exhibited different responses to the inhibitor [35]. CYP2C9*1/*1 individuals exhibited almost a threefold decrease in flurbiprofen clearance, CYP2C9*1/*3 individuals exhibited a twofold reduction in flurbiprofen clearance, and CYP2C9*3/*3 individuals did not exhibit any change in flurbiprofen clearance in response to the inhibitor. The authors pointed out that although the formation clearance of 4′-hydroxy-flurbiprofen was reduced in all genotypes, since f_m was 10% for *3/*3, the effect on flurbiprofen clearance was minimal [35]. Hence, f_m also played an important role, and since f_m changes from CYP2C9*1 through CYP2C9*3, an interplay existed between f_m and genotype, the end result of which is to protect the lower activity variants from DDIs. In addition to CYP2C9, similar results have been obtained for CYP2D6 and CYP2C19, although in those cases, the

resulting polymorphic protein is nonfunctional resulting in an inactive protein [36,37]. Hence, for polymorphic enzymes, genotype of the individuals can affect the degree of DDI observed.

13.3.5 Role of Protein Binding

The binding of drug or inhibitor to plasma proteins or nonspecific binding to microsomal or hepatocyte proteins results in a decrease in the effective drug concentration and the potential to falsely overestimate K_i values. In the case of nonspecific binding to microsomal or hepatocyte proteins, one must carry out extensive experiments to estimate the true unbound concentration so that appropriate corrections can be made. With respect to binding to plasma proteins, some researchers have proposed carrying out incubations with microsomes or hepatocytes suspended in serum [22,38]. Incubations with freshly isolated rat hepatocytes were performed with and without serum to determine if serum incubations were an appropriate system to predict *in vivo* clearance [38]. Sixteen compounds that were cleared mainly by the liver were tested. When incubations were performed in the absence of serum, a poor correlation ($r^2 = 0.55$) of *in vitro* clearance with *in vivo* clearance was obtained. If fraction unbound in serum was determined separately and multiplied by the clearance values, then the r^2 increased to 0.86, thus accounting for the binding of the drug to the serum. This method was then extended to verify DDIs of four combinations of inhibitor and substrate by performing incubations with cryopreserved hepatocytes suspended in 100% serum [22]. First pass hepatic clearance and systemic hepatic clearance were separately predicted using this system. Ketoconazole–terfenadine, ketoconazole–indinavir, and desipramine–quinidine interactions were well correlated with *in vivo* predictions. The accuracy of the predictions was within 0.46–1.5 of the actual *in vivo* values. In this case, no corrections for microsomal binding or serum protein binding were required and since hepatocytes were used, the role of transporters and conjugation enzymes were also represented. These results are contingent on the proper choice of inhibitor concentration.

Since both K_i and [I] values are affected by protein binding, the inclusion of protein binding corrections has been evaluated in a few studies [20]. Forty-five *in vivo* studies were compared with *in vitro* results generated in the investigator's laboratory. In general, use of $K_{i,u}$ improved DDI prediction twofold accuracy by at least 15%. The number of predictions within twofold increased from 56% to 91%; however, $[I]_{avg}$ was total concentration, not a free concentration. While this is a highly successful prediction, the paradox of using $K_{i,u}$ but $[I]_{total}$ is noteworthy. Use of $[I]_{avg,u}$ and $K_{i,u}$ resulted only in a 42% twofold accuracy with mainly underpredictions being responsible for the error. Use of $K_{i,u}$ was particularly important for lipophilic inhibitors with less than 0.06% free fraction (e.g., miconazole and itraconazole). Hence, while unbound concentrations are important, it is still unclear why using both $K_{i,u}$ and $[I]_u$ results in significant underpredictions.

13.3.6 Non-P450 Metabolism and Drug–Drug Interactions

While the principles of *in vitro–in vivo* correlations are the same for non-P450 enzymes as P450 enzymes, the methodology of obtaining the data may be different. The choice of an enzyme system is crucial to the success of the predictions. A recent

review of three test compounds, gemfibrozil, bupropion, and ezetimibe, revealed how the incorrect choice of test system can lead to wrong conclusions [12]. These authors demonstrated that HLMs underpredicted the ability of gemfibrozil to inhibit CYP2C8 in a mechanism-based manner. Since the acyl glucuronide of gemfibrozil was responsible for the interaction, use of human liver microsomes (without uridine 5′-diphospho-glucuronic acid (UDGPA)) prevented the successful prediction of this interaction, whereas use of hepatocytes would have been appropriate for prediction of this DDI [12]. Another drug, bupropion, a CYP2B6 substrate is also a CYP2D6 mechanism-based inhibitor *in vivo*, although *in vitro* human liver microsomal experiments demonstrated a high K_i (low inhibitory potency) for bupropion against CYP2D6. Once again, non-P450 reductases converted the parent to erythro- and threohydrobupropion, both of which are potent mechanism-based inhibitors of CYP2D6. In this instance too, use of hepatocytes would have better predicted the DDI than human liver microsomes [12]. In contrast, ezetimibe is a potent mechanism-based inhibitor of CYP3A4 in human liver microsomes, but when administered to humans, it is extensively directly glucuronidated which prevents the mechanism-based inhibition. Hence, choice of *in vitro* system is crucial in the predictions of non-P450–mediated DDIs.

Some DDIs involving the glucuronosyl transferases (UGT enzymes) and altered drug pharmacokinetics have been reported for compounds such as acetaminophen, codeine, zidovudine, carbamazepine, lorazepam, and propafenone [39]. However, in many cases, these pharmacokinetic changes are of minimal to moderate clinical significance. The reasons underlying the relatively infrequent observation of UGT DDIs have been recently reviewed [40]. The relatively high K_m values of UGT enzymes toward common drugs, which are about 10-fold higher than the typical therapeutic drug concentrations, implies that the velocity is far from being saturated, and hence, a competitive inhibitor that increases the K_m will have minimal impact on the enzyme kinetics. Hence, the continuation of linear kinetics will diminish any impact of the inhibitor on AUC. In addition, due to the high K_m values, the affinity of the UGT to the drug is poor at low substrate concentrations; hence, the hepatic extraction ratios of UGT enzymes are typically lower than observed with the P450 enzymes. A lower hepatic extraction ratio also implies a reduced chance for an adverse DDI reaction. Additionally, the key ratio of $[I]/K_i$ is typically lower for UGT enzymes than P450 enzymes, and multiple UGT enzymes usually catalyze a single substrate. For these reasons, UGT-mediated DDIs are lesser in number than P450–mediated DDIs [40].

Adding to the complexity of predicting UGT DDIs is the lack of specific substrates and inhibitors for these enzymes, although lately selective index reactions appear to have simplified the reaction phenotyping problem. The most commonly employed index substrates/reactions for some of the UGT enzymes are β-estradiol (UGT1A1, 3-glucuronide), 1-naphthol (UGT1A6), propofol (UGT1A9), and naloxone (UGT2B7) [41]. A more comprehensive review of index reactions and substrates for UGTS 1A1, 1A3, 1A4, 1A6, 1A9, 2B7, and 2B15 substrates has been presented, but specific inhibitors were not identified [27].

13.3.7 Role of Drug Pharmacokinetics in Predicting DDIs

As previously alluded to, highly extracted drugs are more susceptible to DDIs, since metabolism can be assumed to be a predominant clearance pathway. This assumption

is not true if biliary excretion of the parent is also a significant clearance pathway. Hence, inhibition of metabolism can cause significant decreases in intrinsic clearance, hepatic clearance, and therefore systemic clearance for highly extracted drugs. However, if a drug has a low extraction ratio to start with then metabolism contributes a minimal amount to its clearance, and therefore further inhibition does not change the pharmacokinetic parameters significantly. For highly extracted drugs, inhibition will predominantly cause C_{max} increases and increased systemic availability, whereas for poorly extracted drugs, inhibition will cause an increase in elimination half-life with no effect on C_{max} [8].

13.3.8 Role of Circulating Metabolites

While most analyses of DDIs restrict themselves to the concentration of the inhibitor, there are situations in which the metabolites of the inhibitors can also possess inhibitory properties. The oft-cited example is that of norfluoxetine, a metabolite of fluoxetine, which is a more potent inhibitor than the parent [8]. In the case of racemic drugs such as fluoxetine and warfarin, the differential inhibitory capacities of S and R enantiomers of parent and metabolites may also impact DDIs. If the circulating concentration of the metabolite is high enough, and the metabolite exhibits a low enough K_i, significant DDIs can result from contributions of the metabolite. The new FDA MIST (Metabolites in Safety Testing) guidance requires the analysis of metabolites greater than 10% of overall exposure (sum of all peak areas) for safety and efficacy. A recent analysis found greater than 94% of drugs have circulating metabolites or are extensively metabolized, hence with potential for DDIs [42]. The role of circulating metabolites may play a factor in the underprediction of DDIs.

13.3.9 Role of Multiple Binding Sites (Allosterism)

Certain P450 enzymes, notably, CYP3A4 and CYP2C9 have multiple catalytic sites within their active sites. In addition, some UGT enzymes also exhibit this property. A number of reviews have provided detailed descriptions of the mechanisms and kinetics governing atypical kinetics [43–46]. Hence, this section only briefly describes the role of atypical kinetics in DDIs.

A direct implication of enzyme allosterism in DDI predictions is the characteristic of substrate-dependent inhibition, wherein the same inhibitor can exhibit differing K_i values depending on the substrate. Thus, reliance on probe substrate results with the compound of interest as the potential perpetrator inhibitor may be tenuous. Substrate-dependent inhibition has been observed for CYP2C9, CYP3A4, and CYP2D6, where K_i values have been found to differ by orders of magnitude depending on the substrate [35,47–49]. One method of addressing this has been to employ multiple substrates for determination of K_i values, as has been done for CYP3A4, since this enzyme is thought to have up to three catalytic sites within its active site [21,50]. Similar considerations may be true for CYP2C9 as well [51]. Substrate-dependent inhibition has also been observed *in vivo* in a randomized, double-blind crossover three phase clinical trial [52]. Nine subjects were orally administered 50-mg mibefradil or 5-mg isradipine or placebo for 3 days followed by the administration of a single dose of 0.25-mg triazolam. Mibefradil, but not isradipine, was found to increase the AUC, plasma concentration, and elimination half-life of triazolam compared to placebo. Hence, although mibefradil,

isradipine, and triazolam are all substrates of CYP3A4, only mibefradil had an effect on triazolam disposition, demonstrating the *in vivo* relevance of substrate-dependent inhibition.

Other types of atypical kinetics may also confound *in vitro–in vivo* correlations and prediction of DDIs, particularly as it relates to the choice of substrate concentrations. For example, in the case of sigmoidal kinetics, use of very low substrate concentrations will lead to the inhibition of the high affinity binding site, while slightly higher concentrations will lead to the inhibition of the lower affinity binding site [51]. In the case of biphasic kinetics, the K_m of interest is usually the higher affinity, lower capacity site; hence, substrate concentrations around the K_{m1} are most appropriate for *in vitro* testing.

In some cases, where competitive inhibition between two substrates is expected heteroactivation can instead be observed. In heteroactivation, the purported inhibitor is actually an activator and increases the turnover of the substrate, while simultaneously undergoing metabolism, for example, dapsone activating flurbiprofen metabolism by CYP2C9 [53]. Thus, determination of whether an interaction actually will occur is confounded by this activation, rather than the expected inhibition.

13.4 CONCLUSIONS

Predicting DDIs is important to the discovery and development of a drug. Unexpected toxicities due to DDIs can lead to adverse patient outcomes, sometimes fatal, causing the withdrawal of a drug from the market. Considering the cost of discovering and bringing to market a new drug, even isolated incidents of DDIs can have potentially serious consequences for both the patient and the manufacturer. Hence, being able to predict (and subsequently cease) development of compounds that have the potential to cause DDIs is crucial to the success of a drug. While the science of predicting DDIs from *in vitro* data has advanced substantially, and the basic principles elaborately elucidated, a 100% prediction success rate has not yet been achieved. Thus, additional research is needed to further refine our capabilities to predict DDIs from *in vitro* data and enhance the drug discovery and development process.

REFERENCES

1. Wienkers LC, Heath TG. Predicting *in vivo* drug interactions from *in vitro* drug discovery data. Nat Rev Drug Discov 2005;4:825–833.
2. Zimmermann M, Duruz H, Guinand O, *et al*. Torsades de pointes after treatment with terfenadine and ketoconazole. Eur Heart J 1992;13:1002–1003.
3. Honig PK, Woosley RL, Zamani K, *et al*. Changes in the pharmacokinetics and electrocardiographic pharmacodynamics of terfenadine with concomitant administration of erythromycin. Clin Pharmacol Ther 1992;52:231–238.
4. Mathews DR, McNutt B, Okerholm R, *et al*. Torsades de pointes occurring in association with terfenadine use. JAMA 1991;266:2375–2376.
5. Zhang L, Zhang YD, Zhao P, *et al*. Predicting drug-drug interactions: an FDA perspective. AAPS J 2009;11:300–306.
6. Food and Drug Administration In Vivo Drug Metabolism/Drug Interaction Studies—Study Design, Data Analysis, and Recommendations for Dosing and Labeling. Available at http://

www.fda.gov/downloads/Drugs/GuidanceComplianceRegulatoryInformation/Guidances/ucm072119.pdf. 1999. (Accessed 2010 June 18).

7. Food and Drug Administration FDA Draft Guidance—Drug Interaction Studies—Study Design, Data Analysis, and Implications for Dosing and Labeling. Available at http://www.fda.gov/downloads/Drugs/GuidanceComplianceRegulatoryInformation/Guidances/ucm072101.pdf. 2006. (Accessed 2010 June 18).
8. Venkatakrishnan K, von Moltke LL, Obach RS, *et al*. Drug metabolism and drug interactions: application and clinical value of *in vitro* models. Curr Drug Metab 2003;4:423–459.
9. Fowler S, Zhang H. *In vitro* evaluation of reversible and irreversible cytochrome P450 inhibition: current status on methodologies and their utility for predicting drug-drug interactions. AAPS J 2008;10:410–424.
10. Huang SM, Temple R, Throckmorton DC, *et al*. Drug interaction studies: study design, data analysis, and implications for dosing and labeling. Clin Pharmacol Ther 2007;81:298–304.
11. Segel IH. Citation-classic—enzyme-kinetics—behavior and analysis of rapid equilibrium and steady-state enzyme-systems. Curr Contents/Life Sci 1987;14:100–160.
12. Parkinson A, Kazmi F, Buckley DB, *et al*. System-dependent outcomes during the evaluation of drug candidates as inhibitors of cytochrome P450 (CYP) and uridine diphosphate glucuronosyltransferase (UGT) enzymes: human hepatocytes versus liver microsomes versus recombinant enzymes. Drug Metab Pharmacokinet 2010;25:16–27.
13. Zhang ZY, Wong YN. Enzyme kinetics for clinically relevant CYP inhibition. Curr Drug Metab 2005;6:241–257.
14. Appiah-Opong R, Commandeur JNM, Vugt-Lussenburg B, *et al*. Inhibition of human recombinant cytochrome P450s by curcumin and curcumin decomposition products. Toxicology 2007;235:83–91.
15. Ring BJ, Binkley SN, Vandenbranden M, *et al*. *In vitro* interaction of the antipsychotic agent olanzapine with human cytochromes P450 CYP2C9, CYP2C19, CYP2D6 and CYP3A. Br J Clin Pharmacol 1996;41:181–186.
16. Ludwig E, Schmid J, Beschke K, *et al*. Activation of human cytochrome P-450 3A4-catalyzed meloxicam 5′-methylhydroxylation by quinidine and hydroquinidine *in vitro*. J Pharmacol Exp Ther 1999;290:1–8.
17. Ito K, Hallifax D, Obach RS, *et al*. Impact of parallel pathways of drug elimination and multiple cytochrome P450 involvement on drug-drug interactions: CYP2D6 paradigm. Drug Metab Dispos 2005;33:837–844.
18. Ito K, Brown HS, Houston JB. Database analyses for the prediction of *in vivo* drug-drug interactions from *in vitro* data. Br J Clin Pharmacol 2004;57:473–486.
19. Brown HS, Ito K, Galetin A, *et al*. Prediction of *in vivo* drug-drug interactions from *in vitro* data: impact of incorporating parallel pathways of drug elimination and inhibitor absorption rate constant. Br J Clin Pharmacol 2005;60:508–518.
20. Brown HS, Galetin A, Hallifax D, *et al*. Prediction of *in vivo* drug-drug interactions from *in vitro* data: factors affecting prototypic drug-drug interactions involving CYP2C9, CYP2D6 and CYP3A4. Clin Pharmacokinet 2006;45:1035–1050.
21. Obach RS, Walsky RL, Venkatakrishnan K, *et al*. The utility of *in vitro* cytochrome P450 inhibition data in the prediction of drug-drug interactions. J Pharmacol Exp Ther 2006;316:336–348.
22. Shibata Y, Takahashi H, Chiba M, *et al*. A novel approach to the prediction of drug-drug interactions in humans based on the serum incubation method. Drug Metab Pharmacokinet 2008;23:328–339.
23. McGinnity DF, Waters NJ, Tucker J, *et al*. Integrated *in vitro* analysis for the *in vivo* prediction of cytochrome P450-mediated drug-drug interactions. Drug Metab Dispos 2008;36:1126–1134.

24. Hisaka A, Ohno Y, Yamamoto T, *et al*. Prediction of pharmacokinetic drug-drug interaction caused by changes in cytochrome P450 activity using *in vivo* information. Pharmacol Ther 2010;125:230–248.
25. Grime K, Riley RJ. The impact of *in vitro* binding on *in vitro–in vivo* extrapolations, projections of metabolic clearance and clinical drug-drug interactions. Curr Drug Metab 2006;7:251–264.
26. Ohno Y, Hisaka A, Suzuki H. General framework for the quantitative prediction of CYP3A4-mediated oral drug interactions based on the AUC increase by coadministration of standard drugs. Clin Pharmacokinet 2007;46:681–696.
27. Miners JO, Mackenzie PI, Knights KM. The prediction of drug-glucuronidation parameters in humans: UDP-glucuronosyltransferase enzyme-selective substrate and inhibitor probes for reaction phenotyping and *in vitro–in vivo* extrapolation of drug clearance and drug-drug interaction potential. Drug Metab Rev 2010;42:189–201.
28. Rowland M, Matin SB. Kinetics of drug-drug interactions. J Pharmacokinet Biopharm 1973;1(6):553–567.
29. Kanamitsu S, Ito K, Sugiyama Y. Quantitative prediction of *in vivo* drug-drug interactions from *in vitro* data based on physiological pharmacokinetics: use of maximum unbound concentration of inhibitor at the inlet to the liver. Pharm Res 2000;17:336–343.
30. Paine MF, Shen DD, Kunze KL, *et al*. First-pass metabolism of midazolam by the human intestine. Clin Pharmacol Ther 1996;60:14–24.
31. Thummel KE, O'Shea D, Paine MF, *et al*. Oral first-pass elimination of midazolam involves both gastrointestinal and hepatic CYP3A-mediated metabolism. Clin Pharmacol Ther 1996;59:491–502.
32. Lown KS, Bailey DG, Fontana RJ, *et al*. Grapefruit juice increases felodipine oral availability in humans by decreasing intestinal CYP3A protein expression. J Clin Invest 1997;99:2545–2553.
33. Galetin A, Gertz M, Houston JB. Contribution of intestinal cytochrome p450-mediated metabolism to drug-drug inhibition and induction interactions. Drug Metab Pharmacokinet 2010;25:28–47.
34. Wang YH, Jones DR, Hall SD. Prediction of cytochrome P450 3A inhibition by verapamil enantiomers and their metabolites. Drug Metab Dispos 2004;32:259–266.
35. Kumar V, Wahlstrom JL, Rock DA, *et al*. CYP2C9 inhibition: impact of probe selection and pharmacogenetics on *in vitro* inhibition profiles. Drug Metab Dispos 2006;34:1966–1975.
36. Hamelin BA, Bouayad A, Methot J, *et al*. Significant interaction between the nonprescription antihistamine diphenhydramine and the CYP2D6 substrate metoprolol in healthy men with high or low CYP2D6 activity. Clin Pharmacol Ther 2000;67:466–477.
37. Uno T, Shimizu M, Yasui-Furukori N, *et al*. Different effects of fluvoxamine on rabeprazole pharmacokinetics in relation to CYP2C19 genotype status. Br J Clin Pharmacol 2006;61:309–314.
38. Shibata Y, Takahashi H, Ishii Y. A convenient *in vitro* screening method for predicting *in vivo* drug metabolic clearance using isolated hepatocytes suspended in serum. Drug Metab Dispos 2000;28:1518–1523.
39. Kiang TK, Ensom MH, Chang TK. UDP-glucuronosyltransferases and clinical drug-drug interactions. Pharmacol Ther 2005;106:97–132.
40. Williams JA, Hyland R, Jones BC, *et al*. Drug-drug interactions for UDP-glucuronosyltransferase substrates: a pharmacokinetic explanation for typically observed low exposure (AUCi/AUC) ratios. Drug Metab Dispos 2004;32:1201–1208.
41. Donato MT, Montero S, Castell JV, *et al*. Validated assay for studying activity profiles of human liver UGTs after drug exposure: inhibition and induction studies. Anal Bioanal Chem 2010;396:2251–2263.

42. Isoherranen N, Hachad H, Yeung CK, *et al*. Qualitative analysis of the role of metabolites in inhibitory drug-drug interactions: literature evaluation based on the metabolism and transport drug interaction database. Chem Res Toxicol 2009;22:294–298.
43. Hutzler JM, Tracy TS. Atypical kinetic profiles in drug metabolism reactions. Drug Metab Dispos 2002;30:355–362.
44. Tracy TS. Atypical enzyme kinetics: their effect on *in vitro-in vivo* pharmacokinetic predictions and drug interactions. Curr Drug Metab 2003;4:341–346.
45. Tracy TS, Hummel MA. Modeling kinetic data from *in vitro* drug metabolism enzyme experiments. Drug Metab Rev 2004;36:231–242.
46. Tracy TS. Atypical cytochrome P450 kinetics, implications for drug discovery. Drugs R D 2006;7:349–363.
47. Ramamoorthy Y, Tyndale RF, Sellers EM. Cytochrome P450 2D6.1 and cytochrome P450 2D6.10 differ in catalytic activity for multiple substrates. Pharmacogenetics 2001;11:477–487.
48. Stresser DM, Blanchard AP, Turner SD, *et al*. Substrate-dependent modulation of CYP3A4 catalytic activity: analysis of 27 test compounds with four fluorometric substrates. Drug Metab Dispos 2000;28:1440–1448.
49. Wang RW, Newton DJ, Liu N, *et al*. Human cytochrome P-450 3A4: *in vitro* drug-drug interaction patterns are substrate-dependent. Drug Metab Dispos 2000;28:360–366.
50. Houston JB, Galetin A. Modelling atypical CYP3A4 kinetics: principles and pragmatism. Arch Biochem Biophys 2005;433:351–360.
51. Korzekwa KR, Krishnamachary N, Shou M, *et al*. Evaluation of atypical cytochrome P450 kinetics with two-substrate models: evidence that multiple substrates can simultaneously bind to cytochrome P450 active sites. Biochemistry 1998;37:4137–4147.
52. Backman JT, Wang JS, Wen X, *et al*. Mibefradil but not isradipine substantially elevates the plasma concentrations of the CYP3A4 substrate triazolam. Clin Pharmacol Ther 1999;66:401–407.
53. Hutzler JM, Hauer MJ, Tracy TS. Dapsone activation of CYP2C9-mediated metabolism: evidence for activation of multiple substrates and a two-site model. Drug Metab Dispos 2001;29:1029–1034.